Fuel 355 (2024) 129357

Contents lists available at ScienceDirect

Fuel

journal homepage: www.elsevier.com/locate/fuel

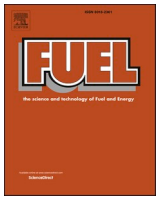

Full Length Article

The potential of dimethyl ether (DME) to meet current and future emissions standards in heavy-duty compression-ignition engines

Patrik Soltic [a,*], Thomas Hilfiker [a], Yuri Wright [a], Gilles Hardy [b], Benjamin Fröhlich [b], Daniel Klein [b]

[a] Automotive Powertrain Technologies Laboratory, Empa - Swiss Federal Laboratories for Materials Science and Technology, Überlandstrasse 129, 8600 Dübendorf, Switzerland

[b] FPT Motorenforschung AG, Schlossgasse 2, 9320 Arbon, Switzerland

ARTICLE INFO

Keywords:
DME combustion
DME injection
Pollutant emission
Exhaust gas treatment
Transient operation

ABSTRACT

Dimethyl Ether (DME, H_3C-O-CH_3) is regarded as a meaningful alternative fuel as it has a comparably high energy density, can easily be stored on vehicles, can be produced via different renewable pathways, has a high Cetane number and is therefore suitable for use in efficient and durable compression ignition engines. Moreover, the DME molecule lacks carbon bonds and due to the inbuilt oxygen atom enables low-sooting diffusion combustion. This study reports on the performance and emission characteristics of a state-of-the-art heavy-duty compression ignition engine with 11 L displacement which was optimized specifically for DME combustion. This includes the adaptation of the fuel supply and injection system as well as the combustion chamber geometry. In addition, the engine is equipped with an electrically driven volumetric pump in the exhaust gas recirculation (EGR) path which gives the freedom to set any desired EGR rate, independently from the pressure ratios across the turbocharger. The experimental results show that DME operation retains the performance on the base Diesel engine (338 kW peak power) while significantly reducing the engine out emissions. The NO_x-soot tradeoff, typical of Diesel applications, basically does not exist anymore so that a desired NO_x level can basically be set without the restrictions of sooting combustion. In addition, the combustion is very complete and very low levels of regulated and non-regulated pollutant emissions can be detected (e.g. for carbon monoxide, DME, methane, benzene, toluene, acetaldehyde, formaldehyde, formic acid). Transient operation is unproblematic and very low emissions can be achieved using the same exhaust gas treatment system as for diesel. Actually, total hydrocarbon, carbon monoxide and particle emission levels of the actual Euro VI and possibly even for the proposed Euro VII on-road legislation could be met without any exhaust gas purification. In terms of tailpipe CO_2 emissions, a reduction of around 11% is possible compared with a diesel-fueled engine.

1. Introduction

In most regions of the world, increasingly stricter greenhouse gas emission limits are imposed across many sectors. Whereas direct electrification is seen as a viable way to increase end-conversion efficiency of duty-cycles with low-power or low-range requirements, chemical energy carriers are very likely to stay dominant for high continuous power and long-range applications. This is mainly because of their superior volumetric and gravimetric energy densities, excellent storability and transportability as well as the potential for fast refueling.

Considerable efforts are underway to bring drop-in replacements for the classical fossil fuels to technical and economical maturity. However, alternative fuels such as hydrogen, ammonia or alternative hydrocarbons are likely to gain importance as they offer certain advantages:

Abbreviations: AdBlue, Trademark for the urea/water solution used in the SCR process, same as AUS 32; aTDC, After Top Dead Center; ATS, After Treatment System; AUS 32, Aqueous Urea Solution (32.5% urea and 67.5% deionized water); BMEP, Brake Mean Effective Pressure; CA, Crank Angle; CNG, Compressed Natural Gas; CUC, Clean Up Catalyst; DEF, Diesel Exhaust Fluid, same as AUS 32; DME, Dimethyl Ether; DOC, Diesel Oxidation Catalyst; DPF, Diesel Particle Filter; EGR, Exhaust Gas Recirculation; FTIR, Fourier Transform Infrared; λ, Air–fuel ratio; LPG, Liquefied Petroleum Gas; MFB, Mass Fraction Burned; NMOG, Non Methane Organic Gases; SCR, Selective Catalytic Reduction; SOI, Start of Injection; THC, Total Hydrocarbons; WHSC, Worldwide Harmonized Stationary Cycle; WHTC, Worldwide Harmonized Transient Cycle.

* Corresponding author.
E-mail address: patrik.soltic@empa.ch (P. Soltic).

https://doi.org/10.1016/j.fuel.2023.129357
Received 16 May 2023; Received in revised form 13 July 2023; Accepted 30 July 2023

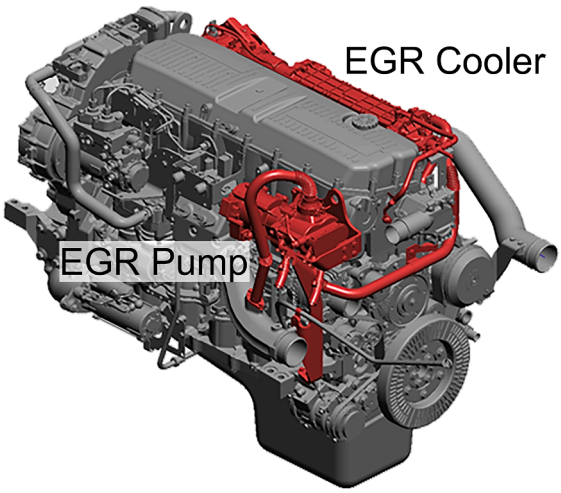

Fig. 1. EGR system consisting of an EGR cooler, an electrically driven EGR pump and respective piping.

Table 1
Main parameters of the engine under consideration.

Base engine	FPT Cursor 11
Bore × stroke	128 mm × 144 mm
Cylinders	6 in line
Nominal peak power (diesel version)	338 kW @ 1900 min^{-1}
Nominal peak torque (diesel version)	2300 Nm @ 970 min^{-1}
Compression ratio	20.5
Piston	H-bowl (see [7])
Common rail pump	Bosch CPN6, oil lubricated, adapted to deliver DME between about 300 and 1300 bar pressure.
Injectors	Bosch CRIN25-L-HD, 145° umbrella angle, 8 orifices with 0.3399 mm diameter
Turbocharger	BorgWarner, VTG
Engine control unit	Bosch MD1 with a calibration link to ETAS INCA
Exhaust gas after treatment	Modular system containing DOC, SCR, CUC and DPF
Exhaust gas recirculation system	Eaton 48 V TVS EGR pump (electrically driven positive displacement pump)
Lubricant	Motorex SAE 0 W/20

- Hydrogen as the easiest chemical energy carrier which can be sustainably produced e.g. from surplus or stranded electricity but there is recent evidence that hydrogen has an surprisingly high indirect short-term global warming potential [1]. This calls for a very careful design of production, transport, storage and conversion technologies to minimize hydrogen emissions.
- Ammonia as a fuel which is straightforward to produce from hydrogen and N_2 abundant in the atmosphere. It has a high toxicity, poor combustion behavior and no global warming potential [2]. Hydrogen addition, e.g. by partial ammonia reforming, may be a way to enhance the poor combustion behavior [3]. Limiting NO_x and especially N_2O emissions remains a major challenge [4]. Ammonia is mainly discussed as a potential fuel for maritime applications [5].
- Alternative hydrocarbons such as synthetic methane, methanol or DME as the simplest hydrocarbons which can be synthesized from H_2 and CO_2, or via direct pathways from biomass or waste [6,7,8].
- More complex fuels with drop-in potential, usually produced by Fischer-Tropsch processes, with deteriorating efficiency for longer chain-length; or by hydrotreatment of bio-oils.

Among the above-mentioned simple chemical energy carriers, DME is the only one with a high cetane number and a low auto-ignition temperature and thus well suited for compression ignition concepts.

Table 2
Main parameters of the engine test bench and engine instrumentation.

AC dynamometer	Horiba Dynas3 HD600 (600 kW / 3,957 Nm peak absorbing power / torque)
Automation system	Horiba STARS Engine
Low-level test bench control	Horiba SPARC
Gaseous emission measurement system 1	Horiba Mexa 7500 DEGR (two emission measurement lines, one EGR measurement line)
Gaseous emission measurement system 2	Gasmet FTIR (calibrated for DME)
Gaseous emission measurement system 3	Siemens LDS (NH_3 measurement)
Particle measurement system 1	AVL Micro Soot Sensor (photoacoustic)
Particle measurement system 2	PMP compliant particle number measurement system with a volatile particle remover, counting all particles above 23 nm
Combustion air	Conditioned (T = 22 °C, rH = 58%)
Air mass flow measurement	ABB Sensyflow P
Fuel flow measurement	Two Coriolis mass flow sensors (Endress + Hauser Cubemass 300)
DME supply	Feed at 26 bar_{abs}, backflow at tank pressure level
Intake channel pressure indication	Keller M5HB sensor
Cylinder pressure indication	Kistler 6045B sensor
Exhaust channel pressure indication	Kistler 4075A sensor (in cooling adapter)
Fuel	DME (purity 99.99 mass%), no additives

Compression ignition internal combustion engines have the advantage of favorable efficiency, the possibility of combining lean combustion, high specific engine power by turbocharging and low pollutant emission levels by using state-of-the-art exhaust gas after treatment. An additional advantage of DME is that it is non-toxic, non-mutagenic, non-carcinogenic, has a very short atmospheric lifetime of less than a week, a low global warming potential of around 1 and is not an ozone-depleting substance [9,10,11].

Especially important for continuous high-power operation such as heavy-duty on– and off-road applications, maritime transport or even for stationary power production is an overall lean operation, which limits thermal load of engine components and guarantees a long engine lifetime. In addition, the volume and mass of the fuel including its storage system is an essential criterion, especially for long-range or long operating-hours applications. Long-haul heavy-duty vehicles are for example typically designed for a range of 1,000 km between refueling. With a classical diesel-based powertrain, around 270 L of fuel are necessary for such a range. Using DME as a diesel replacement fuel, about double the volume is necessary for the same mission. This is feasible for vehicles of this class and much easier and more cost-efficient to place on a vehicle compared to other alternative technologies such as Compressed Natural Gas (CNG) or hydrogen.

DME has several pathways to be produced renewably and it is therefore among the most attractive candidates for renewable fuels in the heavy-duty sector [12]. The suitability of DME as a diesel-replacement fuel was investigated and reported in the past [10,13–15]. Generally speaking, the studies point out the following.

- Compared to Diesel, DME has low lubricity, low viscosity, high compressibility and low volumetric energy density. These points, as well as material compatibility issues of DME, necessitate adaptations of the fuel supply system. The most important modifications include:
  - o The use of an externally lubricated common rail pump or the use of lubricity additives [16,17].
  - o The re-design of the injectors and the common rail pump to guarantee a volumetric flow-rate of about twice the diesel values [18,19,20]. Special attention has to be paid to avoid cavitation.
  - o The reduction of rail pressure levels to minimize compression work.

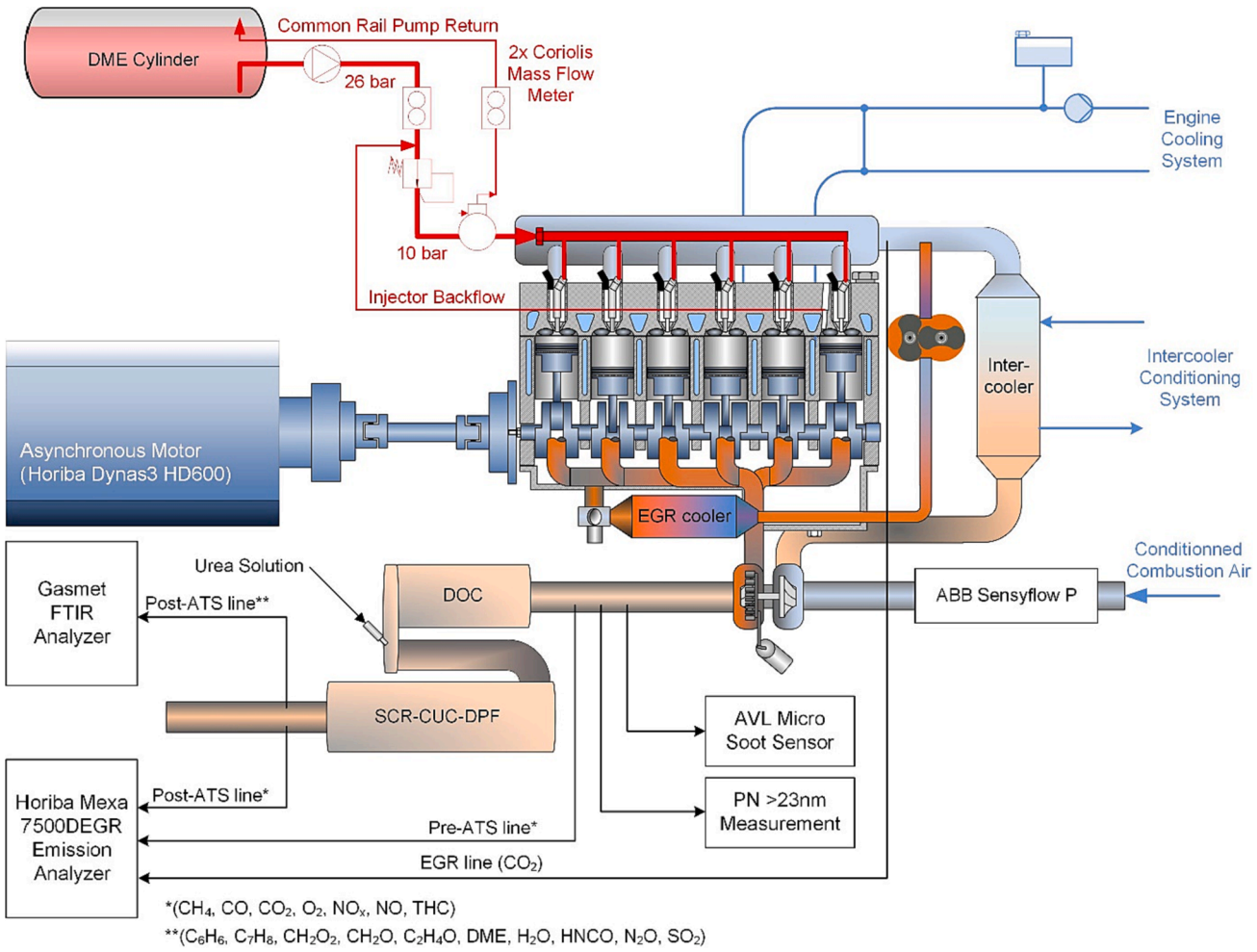

Fig. 2. Schematic of the experimental setup (not shown: ammonia measurement post-ATS).

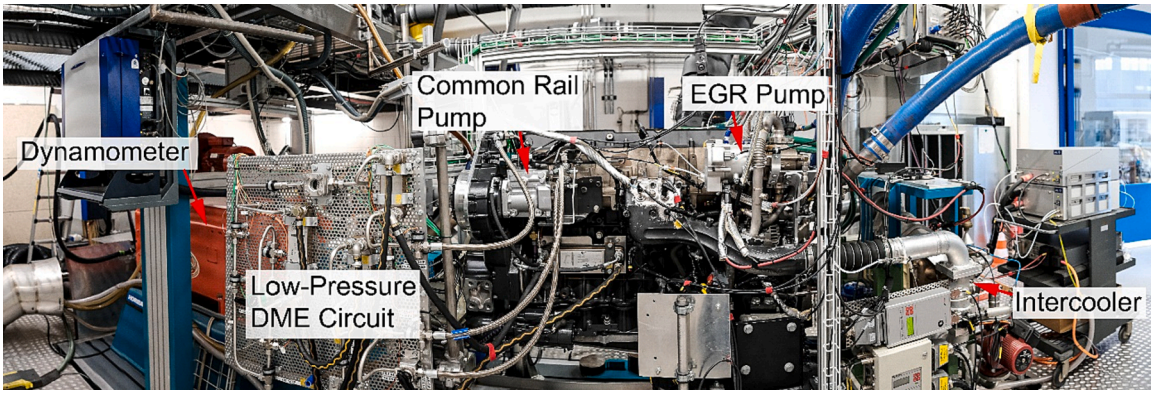

Fig. 3. Configuration of the engine, mounted on the test bench.

- o The re-design of sealing materials to be compatible with DME [17,21–23].
- o The re-design of the tank and fueling infrastructure which, luckily, is very similar to the well-established and cost-efficient systems for Liquefied Petroleum Gas (LPG).

- A reduced rail pressure level does not lead to problems in terms of mixture preparation since the atomization- as well as the evaporation behavior of DME does not require such high rail pressures [24]. However, the DME spray stays liquid for a while at the pressure conditions present in the combustion chamber so that the fuel breakup scheme is very similar to the one of diesel [25,26].
- DME burns practically soot-free in a diffusion-controlled mode. This is not only the case for particle mass emissions, but also for particle number counts. Even in the sub-23 nm range, DME combustion shows extremely low levels, largely independent of EGR [27].
- DME combustion can lead to elevated emissions of unburned hydrocarbons, if the injectors are not properly adapted [28].

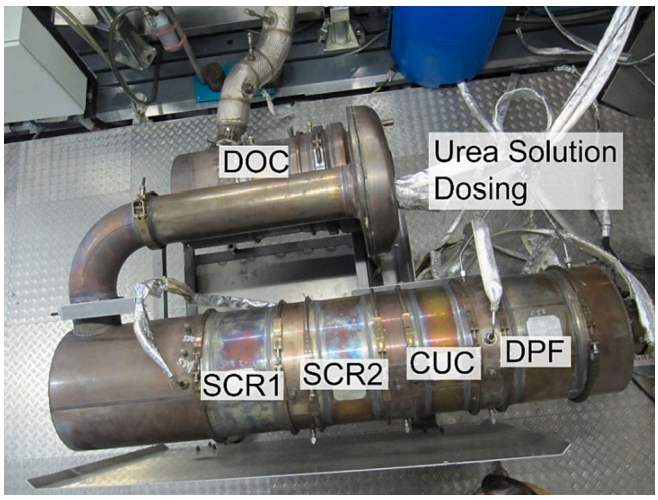

Fig. 4. Configuration of the exhaust gas after treatment system (the system was insulated for the experiments).

- THC emissions are generally low [30] but an increase is reported in some cases at high EGR settings approaching values of 40% [20] where the lack of oxygen starts to play an important role.
- CO levels are lower than for diesel, even at lean conditions [29] but some authors report also increased CO levels [30] and associate this behavior with the lack of boost pressure, if the turbocharger is not adapted the lower exhaust gas enthalpy levels for DME. This is particularly the case when low raw NO_x levels have to be achieved using high amounts of EGR with a classical turbocharger setup.
- Formaldehyde emissions could potentially be higher than for diesel combustion due to the dominant effect of formaldehyde in the combustion process and the oxygen content in DME, especially at low-temperature combustion such as promoted by EGR [31].
- To the authors' best knowledge no studies in the open literature report on the long-term stability of lubricants for DME-operated engines.
- DME is soluble in diesel or biodiesel and such blends can potentially be used in engines [18,32–34]. However, the change of viscosity and lubricity with DME addition remains a challenge. DME can be blended with methanol, which may show slight advantages in terms of engine efficiency [35] in both diffusion-controlled and partially premixed combustion modes. This effect is mainly attributed to a shift of the combustion phasing, if the injection phasing is not adapted. Also, DME may be used as a co-firing fuel to premixed ammonia combustion to overcome the low reactivity of ammonia [36,37].
- The production costs as well as the environmental performance of renewable DME are favorable among other alternatives [38,39,40].

This study presents the optimization of a modern heavy duty full-metal engine specifically for DME and reports thermodynamic and emission measurements for a wide range of operating conditions. Special focus is given to quantify the potential and limitation of DME for reaching the most challenging upcoming pollutant emissions limits such as Euro VII [41] with for example hot emission limits of only 0.09 g/kWh for NO_x in the warm Worldwide Harmonized Transient Cycle. Published studies, specifically looking at engines for commercial use, did not focus on such low emissions levels up to now (e.g. [42,43,44,45]).

2. Methods

This study is based on an FPT Cursor 11 serial-production-engine with specific modifications to run on DME. These modifications include a DME-adapted high-pressure common rail pump, adapted injectors as well as a low-pressure fuel-supply system which is able to deliver DME at 10 bar and return the injectors'- as well as the common rail pump backflows accordingly. The fuel used in all experiments described here is pure DME with a purity of 99.99 mass-% and without any additives. The common rail pump is externally lubricated by engine oil so that it can handle the low fuel lubricity.

In order to have the full freedom to set the exhaust gas recirculation rate independently from the pressure boundary conditions, the engine is equipped with an electrically driven volumetric EGR pump on the high-pressure sides of the turbocharger (see Fig. 1). The high-pressure side is

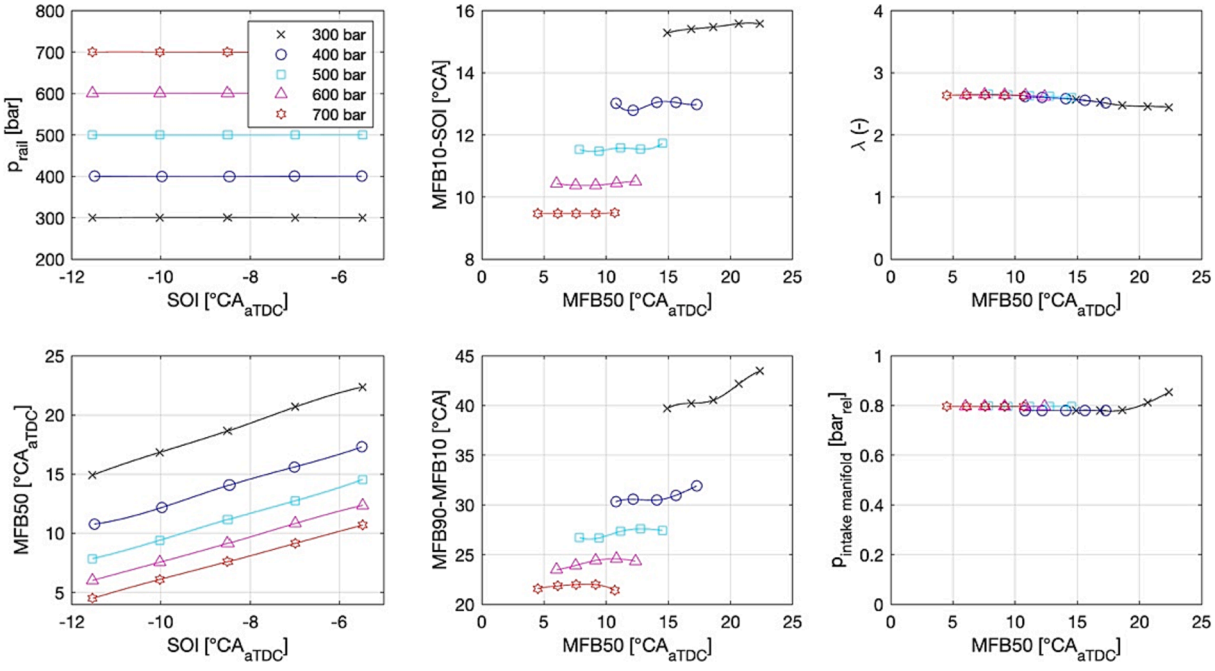

Fig. 5. Effect of start of injection (SOI) and rail pressure variation on combustion (n = 1200 min^{-1}, BMEP = 9.8 bar), no EGR.

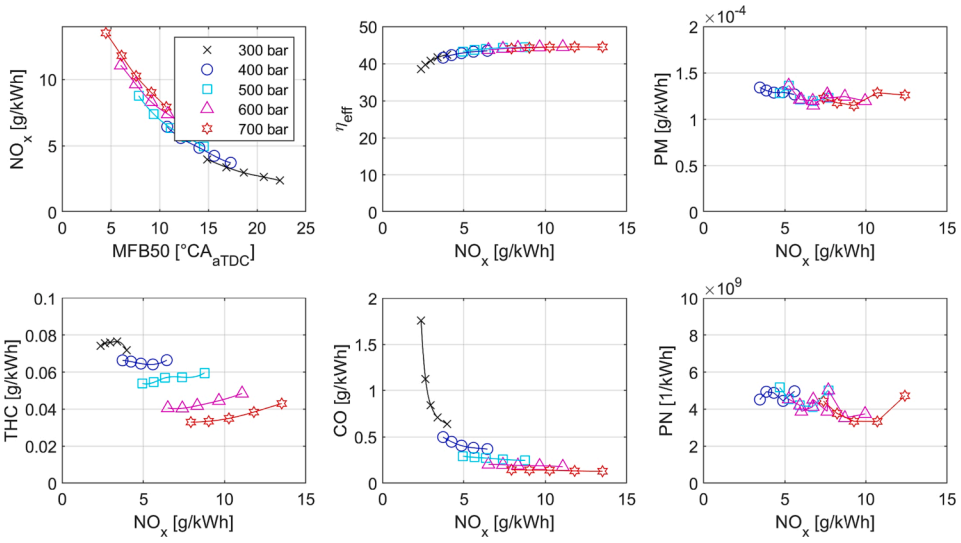

Fig. 6. Effect of start of injection (SOI) and rail pressure variation on efficiency and pollutant emissions pre ATS (n = 1200 min^{-1}, BMEP = 9.8 bar), no EGR.

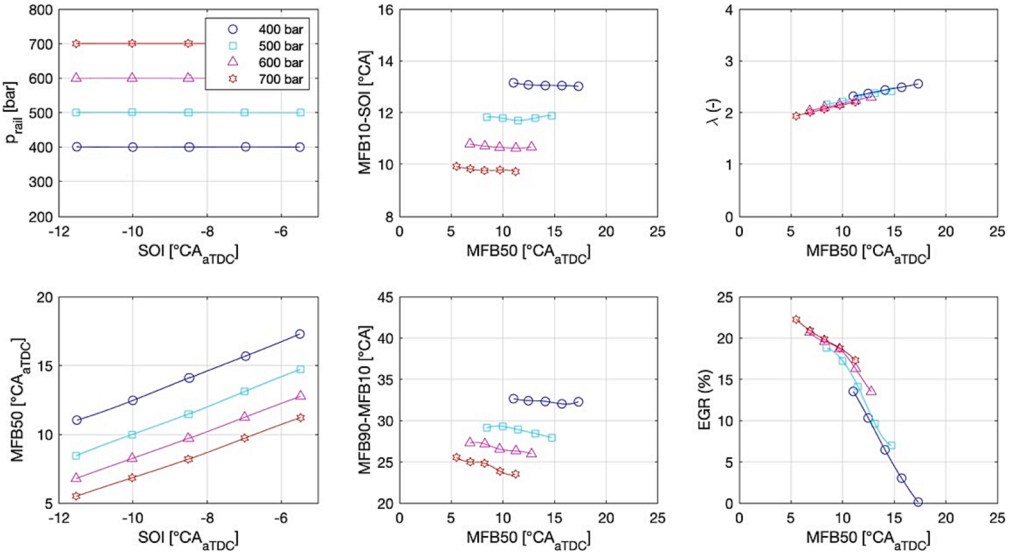

Fig. 7. Effect of start of injection (SOI) and rail pressure variation on combustion (n = 1200 min^{-1}, BMEP = 9.8 bar), EGR adjusted to keep a NO_x level of 4 g/kWh.

chosen to keep the volume flow for the pump small, to not increase the volume flows through the turbocharger and to enable a faster transient control. Table 1 lists the main parameters of the engine.

A state-of-the-art transient engine test bench is used for the experiments. Table 2 lists its main parameters, Fig. 2 shows a schematic of the setup and Fig. 3 shows a picture of the experimental setup.

In order to achieve reproducible conditions the combustion air is conditioned regarding temperature as well as humidity. Fuel mass flow is measured with a double-Coriolis-system which measures the flow to the common rail pump as well as the fuel return to the DME storage tank.

EGR is quantified by measuring the CO_2 concentration in the intake manifold. Regulated emissions are measured with a certification-grade emission bench which samples both the engine's raw emissions as well as the emissions after the exhaust gas after treatment system. In addition, a Fourier-Transform-Infrared-Spectrometer is used to measure gaseous emissions. Typically, automotive FTIR spectrometers are calibrated for Alcohols, Acids and Aldehydes. However, a DME-dedicated spectral emission evaluation method is implemented by the device manufacturer for this project. Not shown in Fig. 2 is the ammonia measurement system which is a non-sampling laser diode spectrometer (i.e. the laser diode and the respective receiver are directly placed in the exhaust gas stream after the exhaust gas after treatment system).

Particle emissions are quantified prior any exhaust gas treatment using a photoacoustic sensor to estimate soot mass as well as a particle number counting system is installed for some experiments.

Thermocouples (type K) and pressure sensors (Keller 33X series) are placed at several points but the full instrumentation is not described here.

The test bench facilitates steady-state as well as dynamic operation of the engine. All time-based data is recorded with a sample rate of 10 Hz using adequate low-pass filtering to meet the Nyquist criterion. For steady-state measurements, the 10 Hz data is averaged over 75 s in post processing.

A modular exhaust gas treatment system (ATS), typically used for diesel exhaust treatment, is used (see Fig. 4). It consists of a Diesel Oxidation Catalyst (DOC) with platinum:palladium coating (2:1), a Selective Catalytic Reduction system (SCR) with Cu- and Fe-zeolite bricks for maximized deNO_x performance with minimal N_2O emissions, a dual layer Clean Up Catalyst (CUC) based on Cu-zeolite/platinum and a porous wall Diesel Particle Filter (DPF). The DPF is deliberately placed

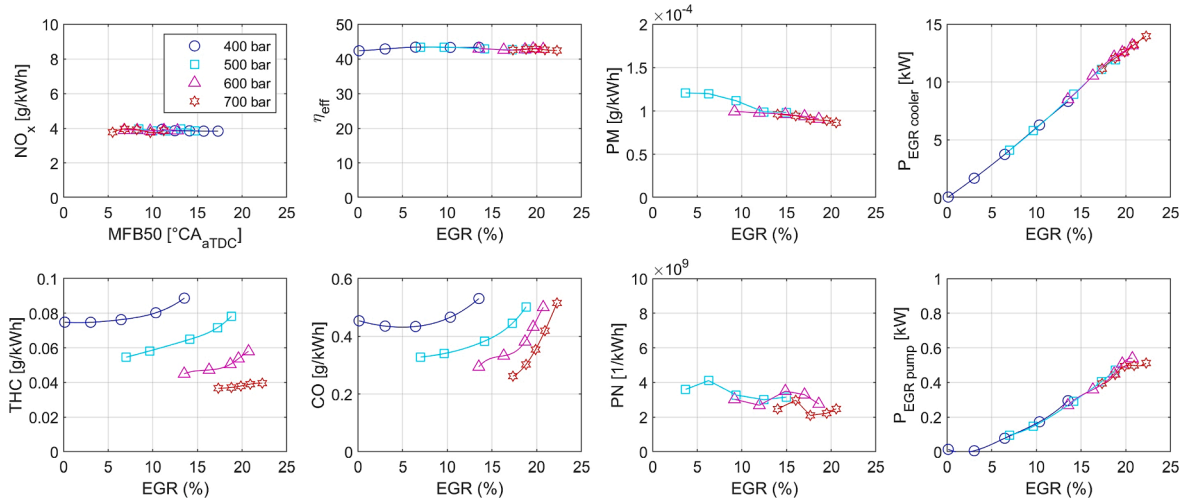

Fig. 8. Effect of start of injection (SOI) and rail pressure variation on efficiency, pollutant emissions pre ATS, EGR pump electrical power and EGR cooler power (n = 1200 min^{-1}, BMEP = 9.8 bar), EGR adjusted to keep a NO_x level of 4 g/kWh.

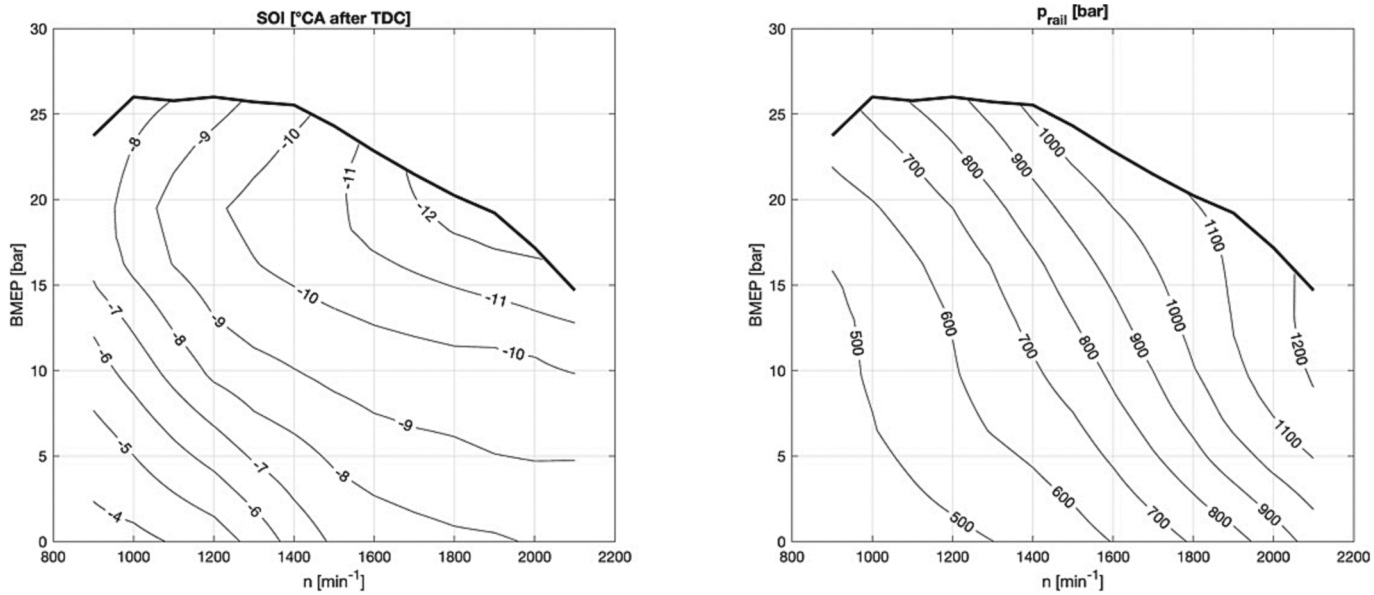

Fig. 9. Start of injection (left) fuel rail pressure settings (right).

at the very end of the system as it is not expected to collect a lot of soot and does therefore not need high exhaust gas temperatures levels for regeneration. In addition, this placement reduces the thermal inertia before the SCR and collects particles caused by urea dosing, which is crucial for the proposed Euro VII particle number emission limits.

3. Results and discussion

Both, steady state as well as transient operation is studied. In a first step, variations of injection phasing, injection pressure and EGR are discussed for a relevant steady-state operating point. Using the findings of this first step, the engine control unit is calibrated accordingly across the entire engine operating map. Finally, the engine is operated in transient conditions.

3.1. Steady state operation

For a 40 tons tractor-semitrailer, the typical engine power demand for driving with 85 km/h on a flat road (i.e. cruising) is around 109 kW. The typical gearbox of such vehicles using this type of engine is laid out such that the engine speed for cruising is 1,200 min^{-1}. This leads to an engine brake torque of 863 Nm for the cruising point or to a Brake Mean Effective Pressure (BMEP) of 9.8 bar for a 11 L engine. Therefore, the variation of parameters in the operating point n = 1200 rpm / BMEP = 9.8 bar is discussed here in detail as this is a very dominant operating point in real life engine operation. Parameter variation experiments were done for a number of other operating points across the engine map as well. The trends were similar so that we omit the detailed discussion of other operating points.

3.2. Injection pressure influence without EGR

In order to evaluate the influence of combustion, efficiency and pollutant emissions on the fuel rail pressure and the injection phasing, a sweep of start of injection (SOI) between −11.5 and −5.5 $°CA_{aTDC}$ and a sweep of rail pressure between 300 and 700 bar is performed for the said operating point. This is done without any exhaust gas recirculation.

Fig. 5 shows the results for combustion parameters as well as for the

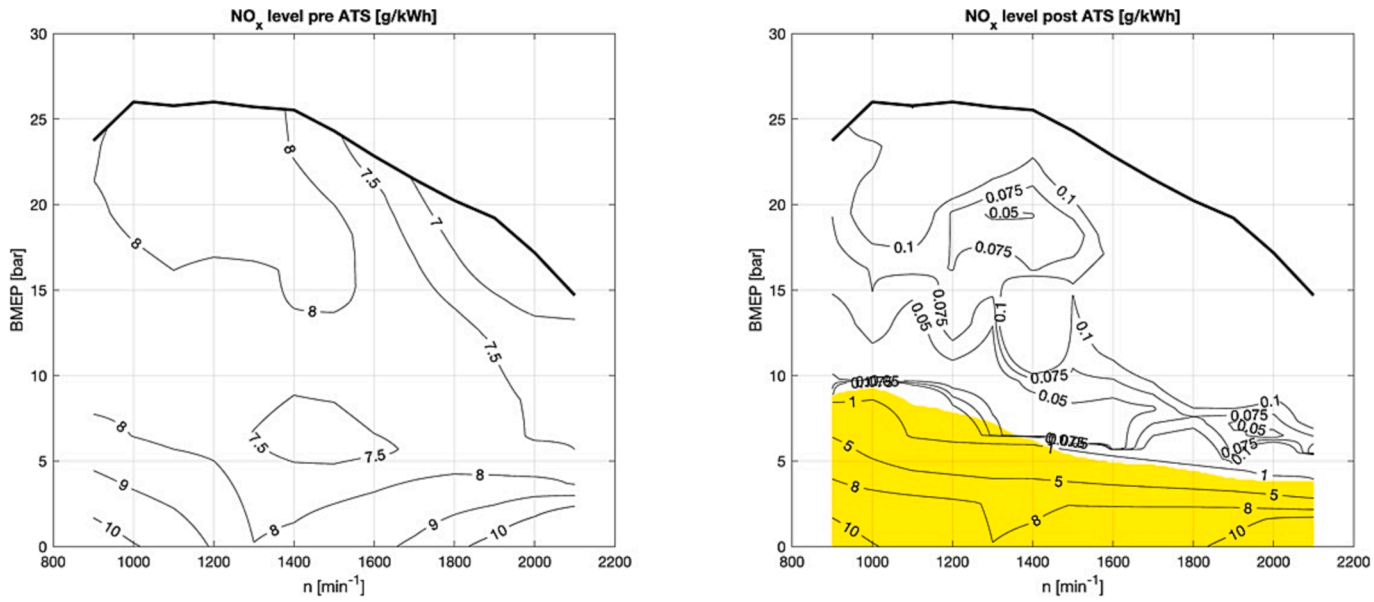

Fig. 10. Engine NO_x emissions map for 8 g/kWh calibration target (left) and resulting NO_x emissions after the exhaust gas after treatment system - the yellow area marks water/urea solution dosing reduction.

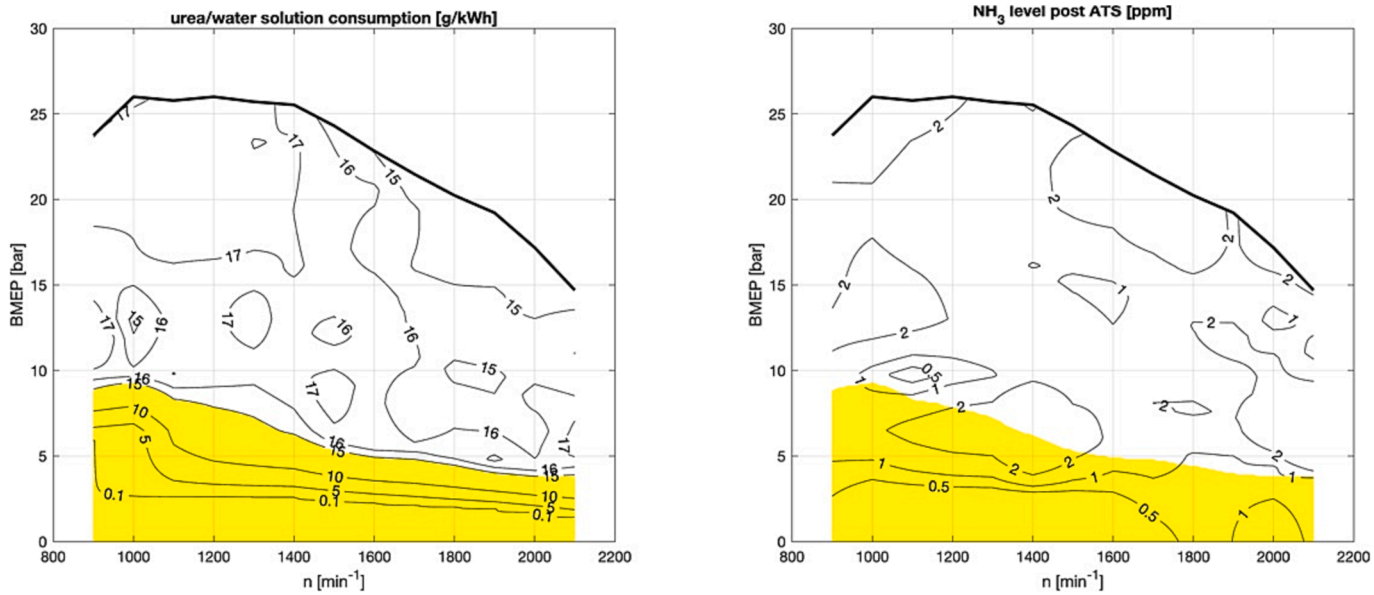

Fig. 11. Urea/water consumption (left) and ammonia emissions after the exhaust gas after treatment system (right) - the yellow area marks part load conditions where the water/urea solution dosing falls below 15 g/kWh.

air–fuel equivalence ratio λ and the intake manifold pressure. The boost was set such that a λ of around 2.5 is present. Increasing rail pressure, however, strongly shortens the ignition delay as the crank angle between SOI and the point of 10% fuel mass burned (MFB10) shows. Not only the ignition delay is influenced by the injection pressure but also the overall combustion duration as the crank angle between 10% and 90% fuel mass burned shows (MFB90-MFB10). As a result, the sweep of SOI between −11.5 and −5.5 °CA_{aTDC} does not lead to a symmetrical sweep in terms of center of combustion (MFB50) for all the investigated rail pressures. It can generally be said that the rail pressure demand is much lower than for a typical diesel case as DME shows a very favorable spray breakup and mixing behavior [7].

Fig. 6 shows the effects on brake thermal efficiency (η_{eff}) as well as on NO_x, total hydrocarbon (THC), particle mass (PM) and particle number (PN) emissions prior any exhaust gas after treatment system. The results show that increasing the injection pressure reduces CO and THC emissions which is an indication for an enhanced spray breakup and mixing process. Increasing the injection pressure increases NO_x slightly which can be explained by a decreasing combustion duration. All in all, an optimal rail pressure can be chosen as a compromise in minimizing CO and THC emissions without sacrificing NO_x levels too much.

Particle mass (PM) as well as particle number (PN) emissions are extremely low and hardly any tendency can be seen. Such low particle emissions are expected as the DME molecule contains oxygen and has no carbon- carbon bonds. The actual European limit values (Euro VI) in the steady-state certification cycle (WHSC) is 0.01 g/kWh for PM and 8e11 1/kWh for PN. For diesel combustion, such limits are only met with highly efficient particle filtration. With DME, the PM and PN emissions are far below the limit values and particle filtration is very

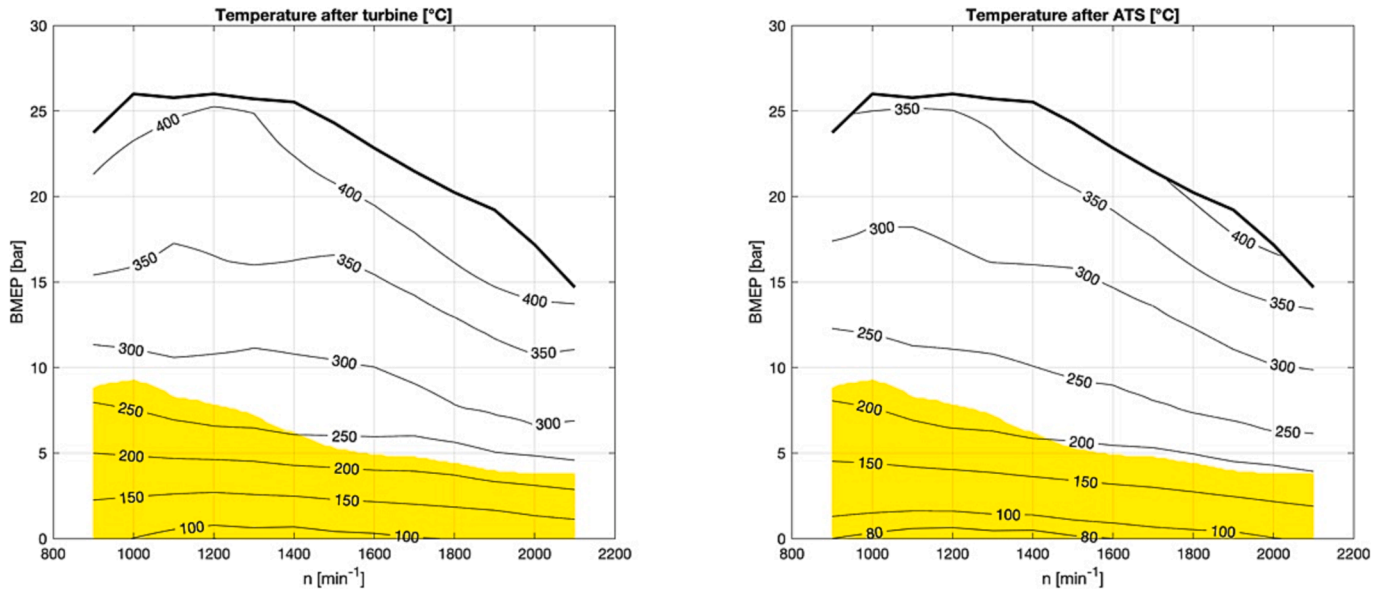

Fig. 12. Temperature levels after turbine (left) and after the exhaust gas after treatment system - the yellow area marks water/urea solution dosing reduction.

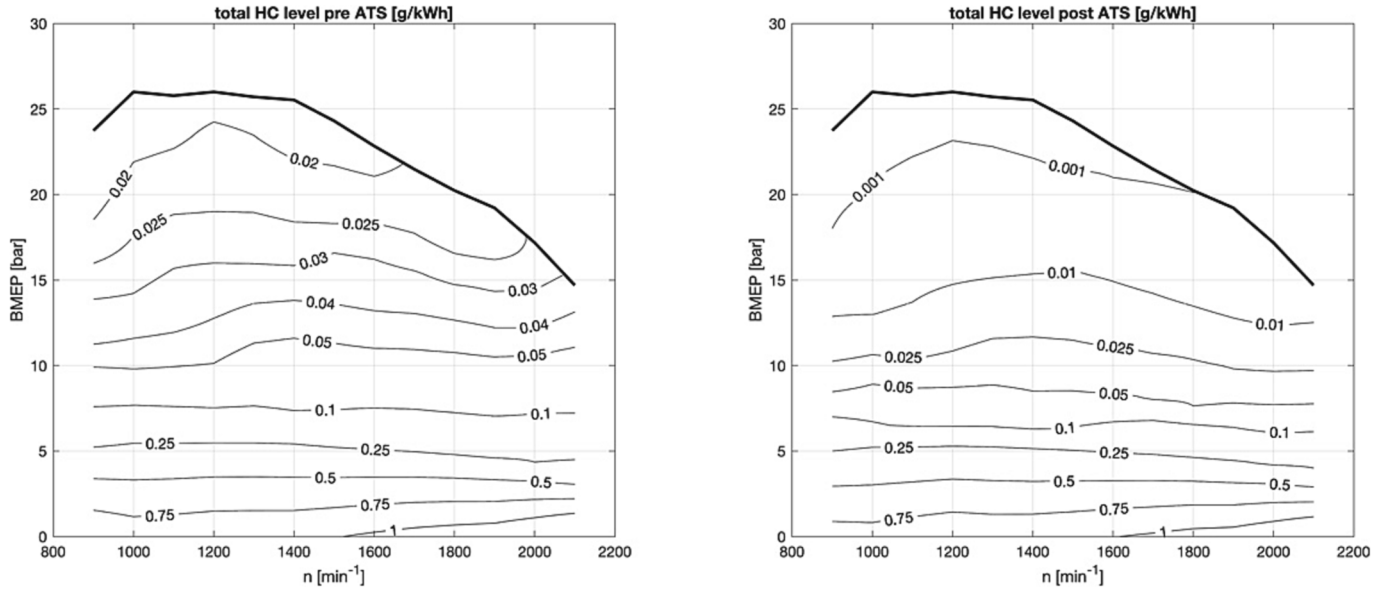

Fig. 13. Total hydrocarbon emissions pre- (left) and post the exhaust gas after treatment system (right).

likely to not be needed to meet even stricter particle limits.

An efficiency-optimal situation can be achieved with NO_x levels of around 8 g/kWh. This means, that the difference between around 8 g/kWh and the requested tailpipe NO_x emission level has to be tackled by a de-NO_x system. A de-NO_x system with 99% efficiency is needed to meet the most stringent standards which are under discussion. Such de-NO_x efficiency levels are reasonable with a modern single stage SCR system as it is used in this project (see Fig. 4). A no-EGR concept has also the advantage that no EGR cooling is needed which reduces the vehicle's radiator size and, as a consequence, has a positive effect on the vehicle's air drag coefficient.

3.3. Injection pressure influence with EGR

Although EGR is not necessarily needed to achieve very low NO_x levels using a highly-efficient deNO_x system, EGR might give advantages in certain situations. If the NO_x emissions have to be cut in half (i.e., from 8 g/kWh to 4 g/kWh), this can only be achieved by delaying combustion when no EGR is applied. With EGR, combustion phasing can be kept at an efficiency-optimal value. To quantify the effect of EGR, a sweep of start of injection (SOI) between −11.5 and −5.5 °CA_{aTDC} and a sweep of rail pressure between 400 and 700 bar is performed for the discussed operating point. The NO_x level is kept at 4 g/kWh by adjusting the amount of EGR.

As Fig. 7 shows, the amount of EGR necessary increases the earlier the combustion is phased and the EGR amount does depend only weakly on the rail pressure level. The combustion intervals between SOI, MFB10 and MFB90 are very similar to the cases without any EGR (Fig. 5): adding EGR does not significantly change the heat release characteristics, albeit the global air excess is reduced. This is presumably due to the oxygen content of the fuel which reduces the deteriorating effect of EGR on diffusion-controlled combustion.

Fig. 8 shows the effects of EGR on brake thermal efficiency (η_{eff}), on NO_x, on total hydrocarbons (THC), on particle mass (PM), on particle

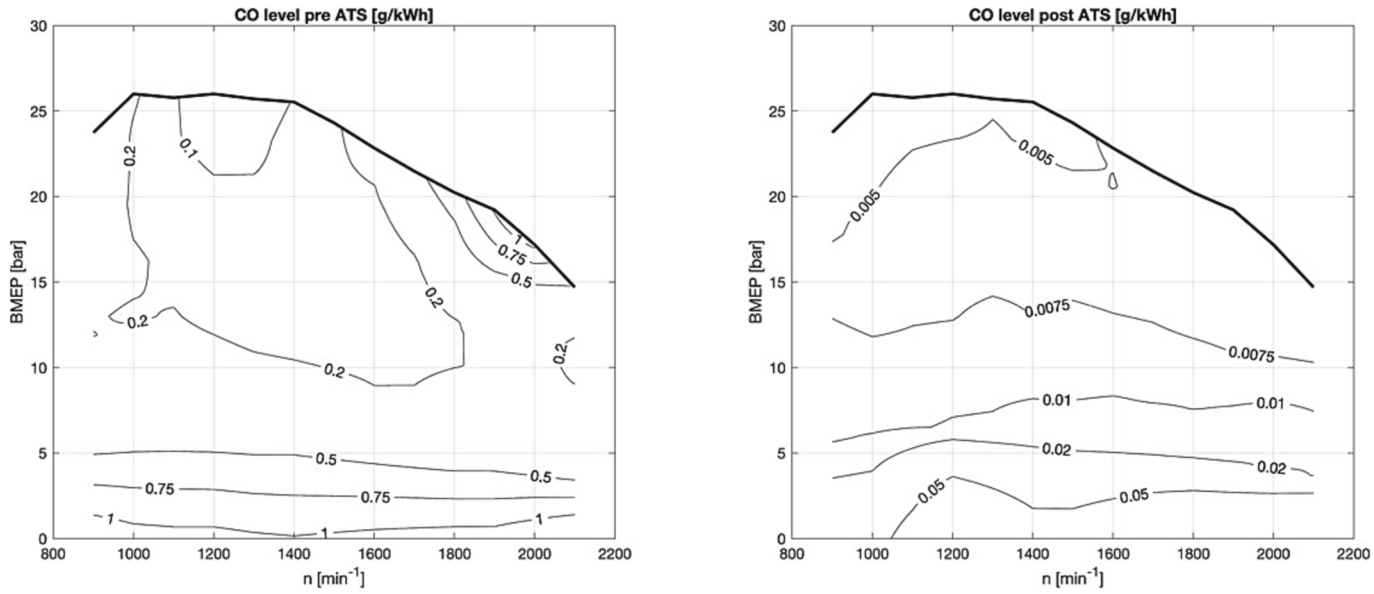

Fig. 14. Carbon monoxide emissions pre- (left) and post the exhaust gas after treatment system (right).

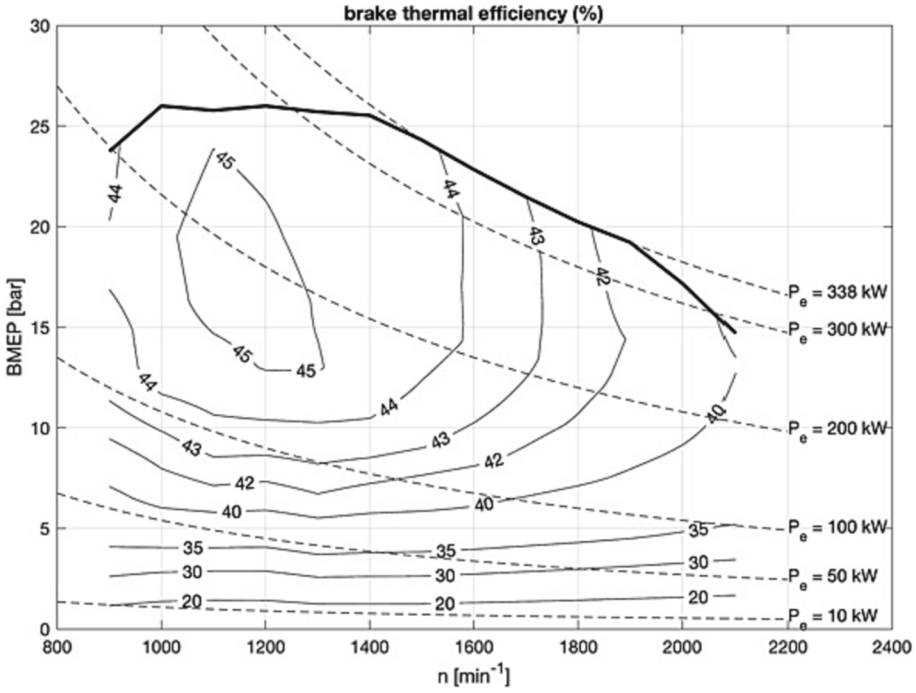

Fig. 15. Brake thermal efficiency.

number (PN) as well as on EGR cooling power and the EGR pump's electric power demand. The results indicate that increasing EGR in combination with increasing rail pressure leads to a reduction in THC and CO emissions but with the obvious disadvantage of EGR cooling power and EGR pump power demands. PM and PN emissions are practically unaffected from EGR and at the same very low levels as discussed earlier for the case without EGR. This means that, unlike for diesel combustion, EGR can be chosen freely without considering negative effects on particle emissions. Brake thermal efficiency levels are only slightly affected by EGR and rail pressure variations and the efficiency values are very similar to the efficiency of the case without any EGR at NO_x levels of 4 g/kWh.

From a technical point of view, it can therefore be concluded that using EGR permanently to reduce engine-out NO_x levels may not be advantageous for the engine configuration considered here as EGR increases the system complexity as well as the engine's cooling power demand. However, depending on the cost of the NO_x reducing agent (known as SCR fluid, AdBlue, DEF or AUS 32), EGR may be an economically feasible solution. Also, EGR is advantageous in situations where the SCR system is not fully functional, e.g. after cold start or at low engine load operation. The EGR layout used here using an electrically driven EGR pump is very beneficial as the EGR rate can be freely set, independently from the pressure boundary conditions around the turbocharger and without the need to modify pressures using a throttle.

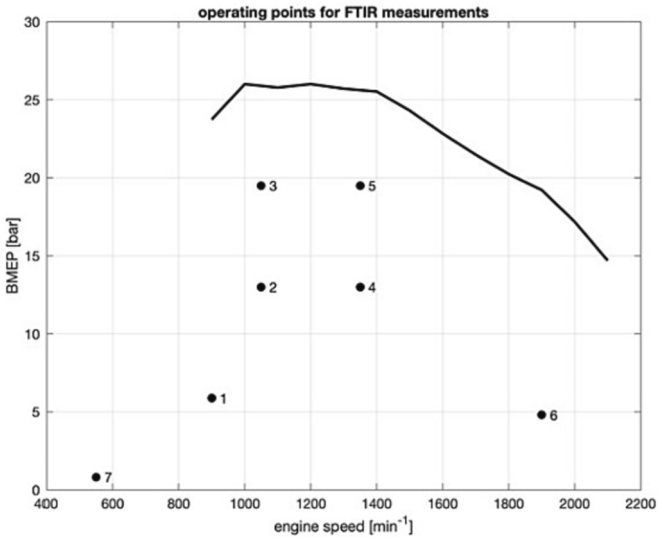

Fig. 16. Operating points for the non-regulated pollutants measurement campaign.

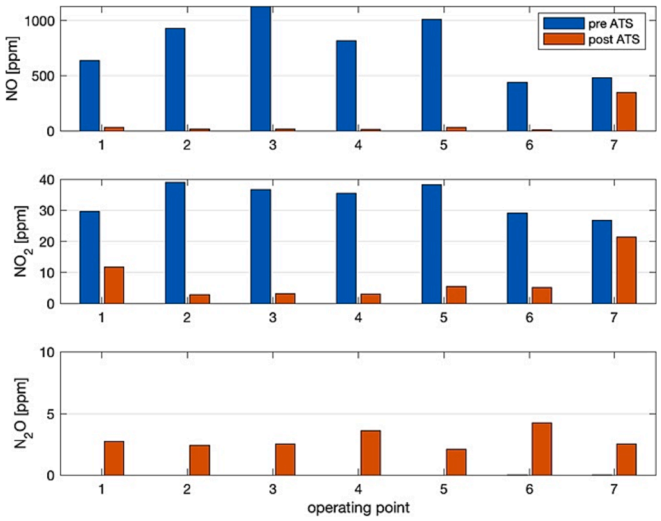

Fig. 17. Pre- and post-ATS levels of oxides of nitrogen oxides for the 7 operating points of Fig. 16.

3.4. Engine map calibration for a NO_x level of 8 g/kWh without external EGR

As discussed earlier, an engine-out NO_x level of 8 g/kWh is a reasonable approach as very low tailpipe NO_x levels can be achieved by established deNO_x systems, the engine's brake thermal efficiency is close to its optimal level and no external EGR is needed. Therefore, the engine is calibrated to a NO_x level of around 8 g/kWh across the entire engine map by adjusting SOI timing and the fuel rail pressure level accordingly while closing the exhaust gas path to set the EGR rate to zero.

Fig. 9 shows the SOI settings for efficiency optimal combustion phasing as well as the fuel rail pressure settings across the engine map. The fuel rail pressure level is chosen as a compromise for low THC and CO emissions, without increasing NO_x emissions too much, and keeping the efficiency as high as possible. This leads to rail pressure levels in the range of 500 bar at low engine power regimes and 1,200 bar around full power conditions.

The resulting cylinder peak pressure levels (not graphically shown) are around 250 bar at peak BMEP conditions which is a result of the comparably high compression ratio of 20.5.

Fig. 10 show the resulting NO_x emissions pre- and post the exhaust gas after treatment system (ATS). Dosing of the urea/water solution is done with the model based FPT control algorithms as used in series production for Diesel applications, but with a specific calibration according the modular system. The ammonia-storage-based control strategy allows high deNO_x efficiency over a single-dosing SCR system. The calibration target of 8 g/kWh raw NO_x emissions is met quite well with the exception of very low load operation where slightly higher NO_x levels are tolerated. After the ATS, very low NO_x levels below 0.1 g/kWh can be measured with the exception of the area marked yellow. This area shows where the dosing of the urea/water solution is reduced in order not to create ammonia emissions and to prevent deposits.

Fig. 11 shows the dosing of the urea/water solution as well as the ammonia slip. The reduction in dosing can clearly be seen, the typical dosing of around 16 g/kWh is gradually reduced to zero at zero load. Doing so, the ammonia emissions after ATS stay at levels around the detection limit of the analyzer across the whole engine map.

The reason why the urea/water dosing has to be reduced is the reduced conversion capability of the ATS with decreasing temperature. As Fig. 12 shows, the capability of the SCR system starts to drop at temperature levels of around 250 °C at turbine exit.

In order to comply with emission regulations, the engine's raw emission levels have to be reduced in such operating regimes, e.g. by applying EGR, late injection, alternative combustion modes such as PCCI, or a combination thereof. Alternatively or additionally, the exhaust gas temperature can be increased by reducing the air excess e.g. by intake airflow or exhaust gas throttling, by fuel dosing to the exhaust or other ATS heating measures. Most of these methods lead to a considerable drop in engine efficiency. Appropriate methods for this specific engine, tailored to the properties of DME, have been investigated and will be reported in a separate publication.

Total hydrocarbon emission levels pre- and post-ATS are shown in Fig. 13. Also here, a reduction in the conversion efficiency can be seen at BMEP levels below around 5 bar. In these regions, the oxidation catalyst has not reached its light off temperature and the engine's HC emissions are not catalytically oxidized. At higher loads, the engine's HC emissions are low anyway and the oxidation catalyst efficiency is good so that very low HC emission levels are detected after the ATS. Similar to the situation with the NO_x emissions, temperature-increasing measures at part load would help increase the oxidation catalyst efficiency. It has to be kept in mind, that the oxidation catalyst employed was developed for diesel and not for DME HC emissions. So, an adapted catalyst formulation might be more efficient. However, the general HC emission level is so low that a highly efficient oxidation catalyst may not be required even for future HC or NMOG emission limits.

Carbon monoxide emissions are usually not an issue in well-designed compression ignition engines. As shown in Fig. 14, this is observed here as well for DME operation: The CO emissions are low across the entire engine map for operation without EGR. The oxidation catalyst is capable of reducing the CO levels even at low load conditions.

Particle mass or particle number emissions in engine map measurements are not reported here as the levels were extremely low and a discussion would not give much insights. However, particle mas- data is given and discusses in section 3.6 which describes transient experiments.

As Fig. 15 shows, the engine's brake thermal efficiency map looks as one would expect for a compression-ignition engine: best efficiency levels at cruising speed and medium-to-high load and a reduction in efficiency at lower load conditions. Above around 6–7 bar bmep, the engine's efficiency is above 40% and the maximum efficiency is slightly above 45%. However, the absolute values are not representative for the engine generation used in this study, as the test engine did not have the most recent friction reduction package. With the most recent design, an increase of the efficiency level of around 1–2 percent-points can be expected.

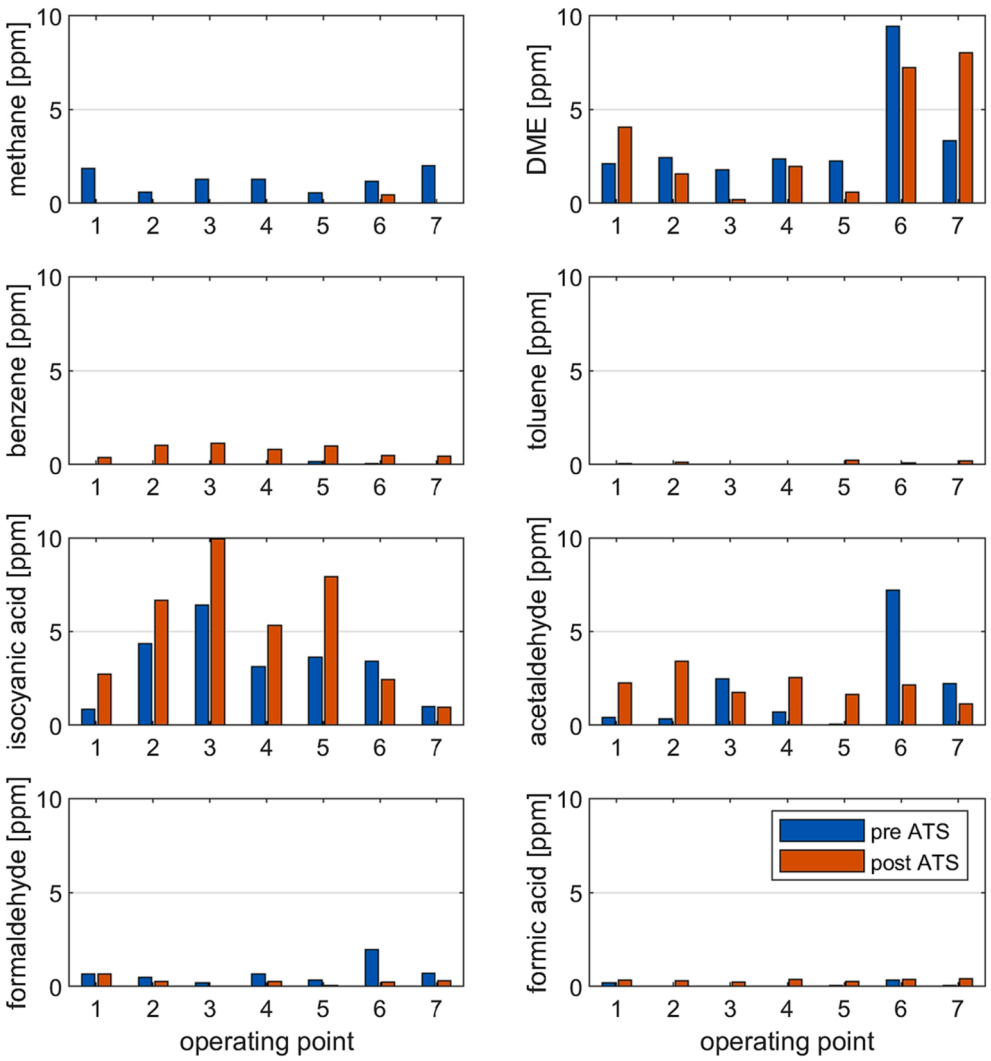

Fig. 18. Pre- and post-ATS emissions for various carbon-containing species for the operating points of Fig. 16.

3.5. Non-Regulated pollutants

Up to now, only regulated pollutant emissions were discussed. In an additional measurement campaign, non-regulated species were measured for seven selected steady-state operating points, including idling conditions. As in the engine map campaign discussed in the previous section, no exhaust gas temperature increasing measures are applied also here and the combustion is calibrated for a NO_x level of 8 g/kWh without EGR. An FTIR analyzer is used for this task (see Fig. 2) which is set up to sample either pre- or post ATS. Concentrations instead of mass-emissions are deliberately discussed in this section as this provides better insight concerning the order of magnitude of the raw values the FTIR instrument detects. As there is no clear precision for FTIR measurements in exhaust gases, mainly because of interference phenomena [46], the measured concentrations allow for a better judgement of the values by the reader.

Fig. 17 shows the pre- and post-ATS results for NO, NO_2 and N_2O concentrations. As expected, the majority of NO_x emissions leaving the engine consist of NO, only about 3…6 vol-% are NO_2. The SCR system is able to reduce a large amount of the NO and the NO_2 emissions with the exception, as previously discussed, when the dosing of the reducing agent has to be reduced because of temperature reasons.

As Fig. 17 shows as well, no N_2O emissions are created by combustion but this greenhouse gas is formed as a side reaction in the ATS. The N_2O formation is expected to increase with temperature for a variety of active catalyst materials ([47,48,49]). This effect is counterbalanced with the used iron-containing catalyst coating [50], as described in section 2. As a net effect, Fig. 17 shows that the N_2O emissions post ATS are very low, independent from the temperature level.

Fig. 18 shows the pre-and post ATS concentrations of specific carbon-containing species. When comparing these results to total hydrocarbon levels one has to keep in mind, that THC is measured with a propane-calibrated flame ionization detector and the concentrations are converted to C_1. So, for example 1 ppm propane (C_3H_8) gives a 3 ppm THC signal. FTIR measurements give the true concentration of a measured species, so for example 1 ppm benzene (C_6H_6) is measured as 1 ppm.

The main findings can be summarized as follows:

- Methane (CH_4) pre ATS concentrations are very low and almost completely removed by the ATS.
- DME (C_2H_6O) emissions are very low and no clear effect of the ATS can be seen.
- Benzene (C_6H_6) is created in very small amount in the ATS.
- Toluene (C_7H_8) is neither detected pre- nor post ATS.
- DME combustion creates a certain amount of Isocyanic acid (HNCO) and the level of these emissions is only slightly affected by the ATS. This indicates, that the net effect of hydrolysis of the engine's HNCO levels and the HNCO levels created from thermolysis of urea [51] have about a net zero effect. Since in diesel combustion, HNCO creation is usually not detected, this seems to be a particular

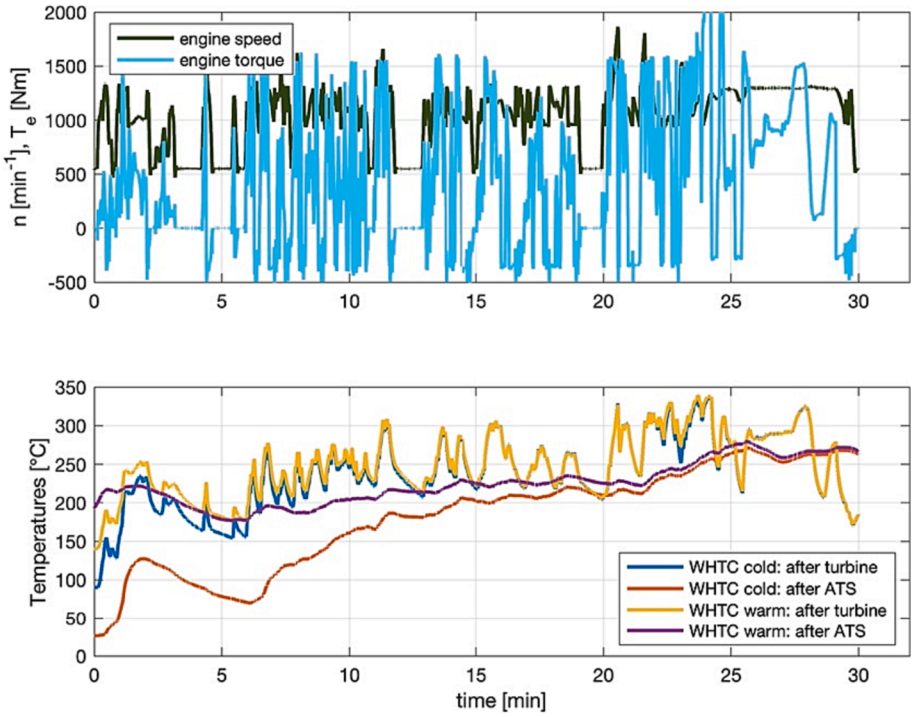

Fig. 19. Engine speed and brake torque (upper plot) and temperature levels after turbine and after ATS (lower plot) for the cold- and the warm-started WHTC.

phenomenon in the DME reaction scheme. Further research to understand how HNCO creation in combustion can be reduced may be needed.

- Acetaldehyde (C_2H_4O) are on a rather low level with an unclear pre-/post ATS trend. The highest pre ATS concentration is measured in the high-speed and low-load operating point #6 where combustion is expected to be the most difficult due to short time for the mixing processes. However, acetaldehyde creation does not seem to be enhanced with DME as it can be observed when alcohols are added to a diffusion-controlled combustion process [52].
- For the combustion without EGR, Formaldehyde (CH_2O) levels are very low, again with the highest pre ATS level at operating point #6. The ATS is able to reduce formaldehyde efficiently, so that post ATS levels are insignificant.
- Formic acid (CH_2O_2) levels are insignificant as well.

3.6. Transient operation

In order to assess how the results from steady-state optimizations transfer to transient engine operation, the Woldwide Harmonized Trasient Cycle (WHTC) is driven on the engine dynamometer. For certification, a WHTC is driven with a cold start, followed by a soak time of 10 min and then a second WHTC is performed. The cold-started cycle contributes 14% to the end results for the actual Euro VI legislation while the proposal for Euro VII foresees that certain limits have to be fulfilled in both the cold and well as the warm cycle.

The effort to perform a full transient engine calibration for DME is too time-consuming for the research project described here where the main goal is to evaluate the general potential of DME. Therefore, the proper steady-state calibration as described in the previous section is adopted but no specific transient or thermal management functions are implemented. Such functions are taken over 1:1 from the engine's diesel calibration instead. As a consequence, the transient results do not represent the best-case scenario for DME but provide valuable evidence of the fuel's performance, anyway.

Fig. 19 shows the engine speed and torque of the driven WHTC versus time as well as the pre- and post ATS temperature levels for the cold- and warm-started cycle. The WHTC represents urban, rural and motorway driving. During the first (urban) part of the cycle, the cold-started WHTC has rather low temperature levels so that the ATS is not fully functional in this section.

Fig. 20 shows work specific pre- and post ATS emissions as well as urea/water dosing versus cycle time. The work-specific emission $\widetilde{m}$ of a species x at time τ is defined as

$$\widetilde{m}_x(\tau) = \frac{\int_{t=0}^{\tau} \dot{m}_x(t)dt}{\int_{t=0}^{\tau} P_e^+(t)dt}$$

With $\dot{m}_x$ being the mass flow of species x and P_e^+ being the mechanical power at the engine's flywheel (set to 0 during motoring phases).

The results show the following.

- Pre ATS NO_x emissions of the cold started cycle are slightly lower than for the warm cycle but both levels are close to the steady-state engine calibration value of 8 g/kWh. The ATS is able to very efficiently reduce the NO_x levels, once the ATS temperature level is sufficient for dosing of the reducing agent. This leads to work-specific NO_x emissions of 0.68 g/kWh for the cold-started and 0.16 g/kWh for the warm cycle. The actual NO_x emission limit for Euro VI is 0.46 g/kWh in the combined cold/hot cycle. This limit can only be met with a de-NO_x system. Both proposed Euro VII NO_x limits of 0.35 g/kWh for the cold cycle and 0.09 g/kWh for the warm cycle are exceeded by a factor of about two. This means that a low-NO_x combustion strategy would have to be chosen at least for the cold-start phase of the system and that the SCR system efficiency would have to be slightly increased by thermal management measures. Given that the transient operation is taken from the engine's diesel calibration it is quite likely, that an increase of SCR efficiency is within reach with software measures only.
- Looking at the THC emissions for the cold-started WHTC, an interesting behaviour can be observed: in the first period up to about two minutes cycle time, the emissions post ATS are lower than pre ATS. After this time period, the emissions post ATS exceed the pre ATS levels. This indicates that the ATS has a THC storage effect at low

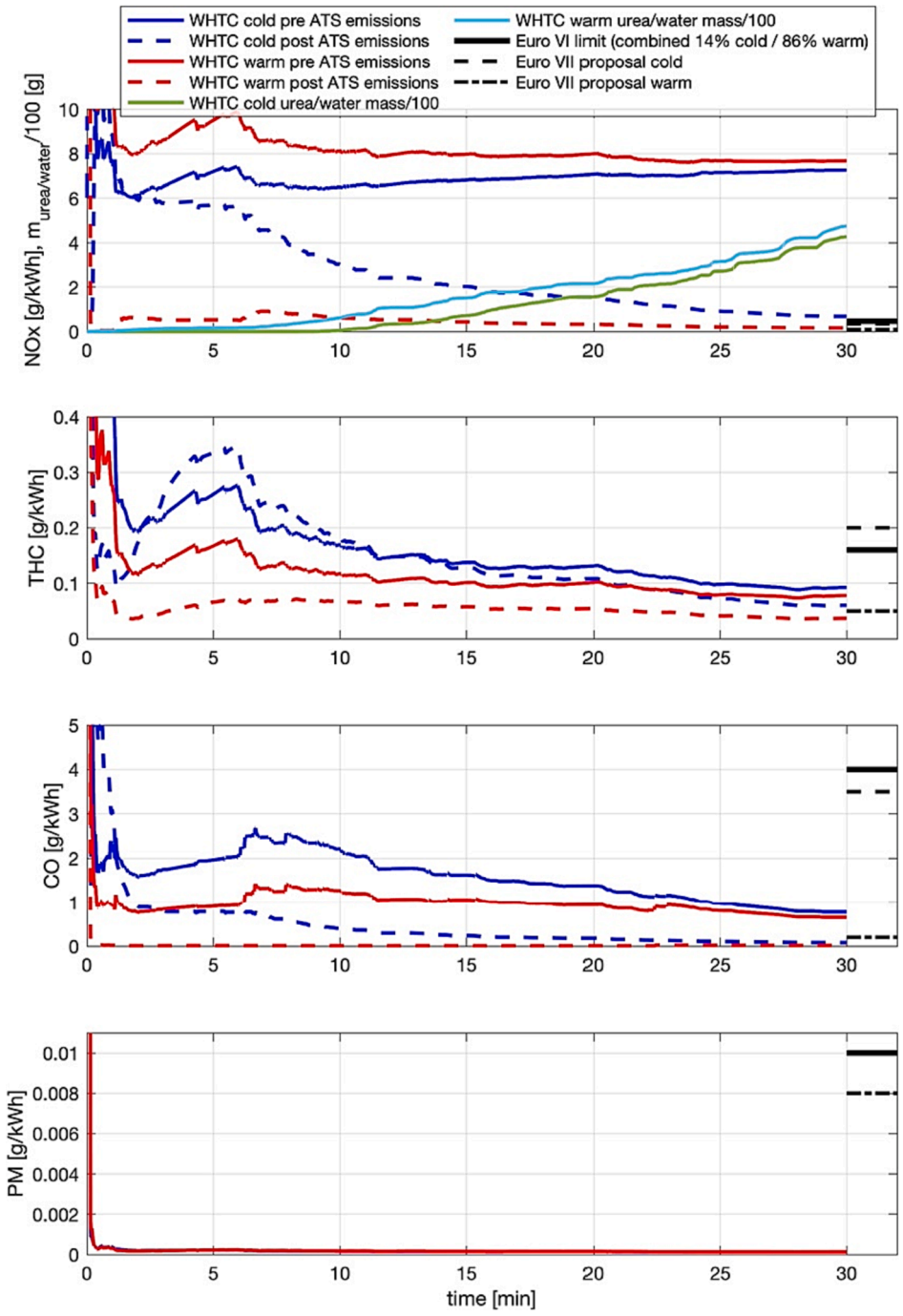

Fig. 20. Pre- and post ATS NO_x, THC, CO emission, injected urea/water mass and pre ATS particle mass for the cold- and the warm-started WHTC.

temperature levels. After a certain temperature level is reached, THC is released and once the oxidation catalyst's light-off temperature is met, the catalytic THC oxidation takes place. Overall, as also seen in the engine map experiments (Fig. 13), the THC conversion efficiency of this particular oxidation catalyst is not particularly high at around 50%. However, this still leads to low work-specific THC emissions of 0.06 g/kWh for the cold-started and 0.03 g/kWh for the warm cycle. The acutal THC emission limit for Euro VI is 0.16 g/kWh in the combined cold/hot cycle. These THC limits are met even pre ATS. Also the proposed Euro VII limits for Non-Methane Organic Gases (NMOG) of 0.2 mg/kWh for the cold and 0.05 g/kWh for the warm cycle are met pre ATS.

- CO emissions levels are below 1 g/kWh pre ATS and 0.08 g/kWh post ATS for the cold-started and 0.02 g/kWh for the warm cycle. The catalytic oxidation is very efficient. The acutal CO emission limit for Euro VI is 4 g/kWh in the combined cold/hot cycle. As Fig. 20 shows, the Euro VI CO limits are met even pre ATS. Also the proposed Euro VII CO limits of 3.5 g/kWh for the cold and 0.2 g/kWh for the hot are easily met pre ATS.
- Pre-ATS particle mass (PM) emissions, measured with a Micro Soot Sensor, are on an extremely low level. The PM measurements are practically identical for the warm- and for the cold cycle and at 0.13 mg/kWh. The tailpipe PM emission limit for Euro VI is 10 mg/kWh in the combined cold/hot cycle. As for THC and CO, the Euro VI PM

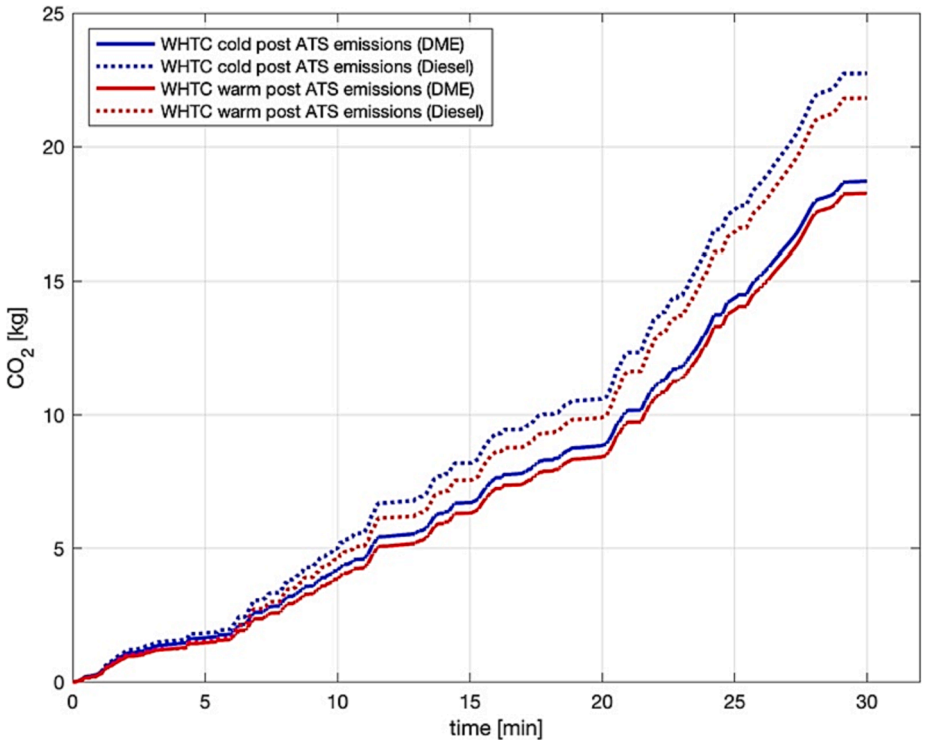

Fig. 21. Cumulated tailpipe CO_2 emission for the cold- and the warm-started WHTC for the engine operated on DME and for the serial-production engine in Diesel operation.

emission limits are met pre ATS. Also the proposed Euro VII PM limit of 8 mg/kWh (both for the cold and the warm cycle) is easily met.

Fig. 21 shows the evolution of CO_2 produced for the cold- as well as for the warm-started WHTC. Besides the results for DME, Fig. 21 shows the results for the serial-production Euro VI certified Diesel version of this engine. DME shows a reduction of tank-to-tailpipe CO_2 emissions of about 12% in the cold-started and of about 10% in the warm-stared WLTC. This reduction in tailpipe CO_2 emissions can of course be further expanded by using renewable DME, as discussed in the introduction. However, already a reduction of tailpipe CO_2 emissions by 11% may be attractive for heavy duty applications as the potential to increase engine efficiency further is rather limited because of thermodynamic reasons. Therefore, the use of a clean-burning low-carbon high-cetane fuel is certainly attractive.

4. Conclusions

DME proves to be an ideal fuel for heavy-duty compression ignition engines at it offers practically particle-free combustion by effectively eliminating the soot/NO_x trade-off inherent to Diesel combustion. This gives the freedom to set the NO_x level the engine emits depending on the conversion efficiency of the ATS, cost considerations taking into account the price of the SCR fluid and the required tailpipe emission levels. The electrically driven volumetric EGR pump proves to be a valuable approach to set the EGR rate at any desired level, independent from the pressure boundary conditions across the turbocharger. THC, CO as well as levels of non-regulated emissions are very low for a proper combustion system layout. Particle emissions are far below any existing emission limits so that particles basically need not be considered when the combustion strategy is optimized.

The excellent results achieved at steady-state operation are fully transferred to transient operation. Looking at current Euro VI emission limits, CO, THC and particle emission limits are met without the need for exhaust gas after treatment, only a de-NO_x system is needed. Even the very strict Euro VII limits proposed for CO, NMOG, CH_4 and PM are met with the comparably simple engine calibration used in this project. A reduction of the pre ATS emission level or a better calibration of the SCR functions may however be required to meet the proposed Euro VII NO_x limits of 0.35 g/kWh (cold WHTC) and 0.09 g/kWh (warm WHTC).

In terms of CO_2 emissions, DME offers an advantage of at least 10% over Diesel with the potential of extending the ecological potential even further by using renewable DME, which can be produced in simpler processes than renewable Diesel-substitutes.

The fair energy density of DME in combination with the numerous pathways for sustainable production, the diesel-like high conversion efficiency together with the possibility to meet extremely strict emission regulations with a comparably low technical effort for exhaust gas purification render DME a very attractive fuel for a number of applications in the future. The authors therefore recommend that DME should be considered seriously as a sustainable future fuel for the heavy-duty on– and off-road sector. DME has the technical, economic and ecological potential to ideally complement other sustainable fuels such as hydrogen, methanol, methane or ammonia. During the experiments described in this paper, no issues were found with the externally lubricated DME pump. However, a thorough assessment of the durability of such a pump over the desired lifetime has to be made before this technology can be industrialized.

CRediT authorship contribution statement

Patrik Soltic: Conceptualization, Formal analysis, Funding acquisition, Project administration, Supervision, Visualization, Writing – original draft, Writing – review. **Thomas Hilfiker:** Data curation, Investigation, Software, Visualization. **Yuri Wright:** Software, Editing. **Gilles Hardy:** Conceptualization, Data curation, Formal analysis, Investigation, Software. **Benjamin Fröhlich:** Project administration, Supervision. **Daniel Klein:** Conceptualization, Funding acquisition, Project administration, Supervision.

Declaration of Competing Interest

The authors declare that they have no known competing financial interests or personal relationships that could have appeared to influence the work reported in this paper.

Data availability

The authors do not have permission to share data.

Acknowledgments

The authors gratefully acknowledge the financial support of the Swiss Federal Office of Energy (contract number SI/501794-01). This project would not have been possible without the technical support of Michael Harter and Theo Kraus of FPT Motorenforschung as well as of Roland Graf, Daniel Schreiber, Hugo Ehrensperger and Roland Spühler of Empa.

References

[1] Ocko IB, Hamburg SP. Climate consequences of hydrogen emissions. Atmos Chem Phys 2022;22:9349–68. https://doi.org/10.5194/acp-22-9349-2022.
[2] Wüthrich S, Cartier P, Süess P, Schneider B, Obrecht P, Herrmann K. Optical investigation and thermodynamic analysis of premixed ammonia dual-fuel combustion initiated by dodecane pilot fuel. Fuel Commun 2022;12:100074. https://doi.org/10.1016/j.jfueco.2022.100074.
[3] Mashruk S, Okafor EC, Kovaleva M, Alnasif A, Pugh D, Hayakawa A, et al. Evolution of N2O production at lean combustion condition in NH3/H2/air premixed swirling flames. Combust Flame 2022;244:112299. https://doi.org/10.1016/j.combustflame.2022.112299.
[4] Li J, Lai S, Chen D, Wu R, Kobayashi N, Deng L, et al. A Review on Combustion Characteristics of Ammonia as a Carbon-Free Fuel. Front Energy Res 2021;9:1–15. https://doi.org/10.3389/fenrg.2021.760356.
[5] Stolz B, Held M, Georges G, Boulouchos K. Techno-economic analysis of renewable fuels for ships carrying bulk cargo in Europe. Nat Energy 2022;7:203–12. https://doi.org/10.1038/s41560-021-00957-9.
[6] Merkouri L-P, Ahmet H, Ramirez Reina T, Duyar MS. The direct synthesis of dimethyl ether (DME) from landfill gas: A techno-economic investigation. Fuel 2022;319:123741. https://doi.org/10.1016/j.fuel.2022.123741.
[7] Schirru A, D'Errico G, Lucchini T, Zhou Q, Hardy G, Soltic P, et al. Combustion Modeling in a Heavy-Duty Engine Operating with DME Using Detailed Kinetics and Turbulence Chemistry Interaction. SAE Tech Pap 2022. https://doi.org/10.4271/2022-01-0393.
[8] Ateka A, Rodriguez-Vega P, Ereña J, Aguayo AT, Bilbao J. A review on the valorization of CO2. Focusing on the thermodynamics and catalyst design studies of the direct synthesis of dimethyl ether. Fuel Process Technol 2022;233. https://doi.org/10.1016/j.fuproc.2022.107310.
[9] Good DA, Francisco JS, Jain AK, Wuebbles DJ. Lifetimes and global warming potentials for dimethyl ether and for fluorinated ethers: CH3OCF3 (E143a), CHF2OCHF2 (E134), CHF2OCF3 (E125). J Geophys Res Atmos 1998;103:28181–6. https://doi.org/10.1029/98JD01880.
[10] Arcoumanis C, Bae C, Crookes R, Kinoshita E. The potential of di-methyl ether (DME) as an alternative fuel for compression-ignition engines: A review. Fuel 2008;87:1014–30. https://doi.org/10.1016/j.fuel.2007.06.007.
[11] N/A. Ozone-Depleting Substances. United States Environ Prot Agency 2022. https://www.epa.gov/ozone-layer-protection/ozone-depleting-substances.
[12] Styring P, Dowson GRM, Tozer IO. Synthetic Fuels Based on Dimethyl Ether as a Future Non-Fossil Fuel for Road Transport From Sustainable Feedstocks. Front Energy Res 2021;9:1–22. https://doi.org/10.3389/fenrg.2021.663331.
[13] Thomas G, Feng B, Veeraragavan A, Cleary MJ, Drinnan N. Emissions from DME combustion in diesel engines and their implications on meeting future emission norms: A review. Fuel Process Technol 2014;119:286–304. https://doi.org/10.1016/j.fuproc.2013.10.018.
[14] Park SH, Lee CS. Applicability of dimethyl ether (DME) in a compression ignition engine as an alternative fuel. Energy Convers Manag 2014;86:848–63. https://doi.org/10.1016/j.enconman.2014.06.051.
[15] Patten J. Dimethyl ether fuel literature review. NRC Publications Archive 2016. https://doi.org/10.4224/23000192.
[16] Sugiyama K, Kajiwara M, Fukumoto M, Mori M, Goto S, Watanabe T. Lubricity of liquefied gas assessment of multi-pressure/temperature high-frequency reciprocating rig (MPT-HFRR) -DME fuel for diesel. SAE Tech Pap 2004. https://doi.org/10.4271/2004-01-1865.
[17] Pal M, Kumar V, Kalwar A, Mukherjee NK, Agarwal AK. Prospects of Fuel Injection System for Dimethyl Ether Applications in Compression Ignition Engines. Springer Singapore; 2021. https://doi.org/10.1007/978-981-16-1513-9_2.
[18] Baeck B, Lim O. Performace Improvement of Independent High Pressure Pump for DME. Int J Automot Technol 2022;23:1365–71. https://doi.org/10.1007/s12239.
[19] Mukherjee NK, Valera H, Unnithan S, Kumar V, Dhyani V, Mehra S, et al. Feasibility study of novel DME fuel injection Equipment: Part 1- fuel injection strategies and spray characteristics. Fuel 2022;323:124333. https://doi.org/10.1016/j.fuel.2022.124333.
[20] Hara T, Shimazaki N, Yanagisawa N, Seto T, Takase S, Tokumaru T, et al. Study of DME diesel engine for Low NOx and CO2 emission and development of DME trucks for commercial use. SAE Tech Pap 2011. doi: 10.4271/2011-01-1961.
[21] Kass MD, Daw C. Compatibility of Dimethyl Ether (DME) and Diesel Blends with Fuel System Polymers: A Hansen Solubility Analysis Approach. SAE Int J Fuels Lubr 2016;9:71–9. https://doi.org/10.4271/2016-01-0835.
[22] Li GB, Zhou LB. Experimental research on the resistance of rubber materials to dimethyl ether. Proc Inst Mech Eng Part D J Automob Eng 2008;222:975–8. https://doi.org/10.1243/09544070JAUTO758.
[23] Sari TI, Saputra AH, Bismo S, Maspanger DR. Deproteinized natural rubber grafted with polyacrylonitrile (PAN)/polystirene (PS) and degradation of its mechanical properties by dimethyl ether. Int J Technol 2020;11:15–25. https://doi.org/10.14716/ijtech.v11i1.1942.
[24] Konno M, Chiba K, Okamoto T. Experimental and numerical analysis of high pressure DME spray. SAE Tech Pap 2010. doi: 10.4271/2010-01-0880.
[25] Oguma M, Hyun G, Goto S, Konno M, Kajitani S. Atomization characteristics for various ambient pressure of dimethyl ether (DME). SAE Tech Pap 2002. doi: 10.4271/2002-01-1711.
[26] Sasaki S, Kato M, Yokota T, Konno M, Gill D. An Experimental Study of Injection and Combustion with Dimethyl Ether. SAE Tech Pap 2015;2015-April. doi: 10.4271/2015-01-0932.
[27] Pélerin D, Gaukel K, Härtl M, Wachtmeister G. Nitrogen Oxide Reduction Potentials Using Dimethyl Ether and Oxymethylene Ether in a Heavy-Duty Diesel Engine. SAE Tech Pap 2020; 2020-Janua:1–14. doi: 10.4271/2020-01-5084.
[28] Salsing H. DME as a Sustainable Heavy-Duty Diesel Alternative - from a combustion perspective. DME Sustain. Mobil. Work. Aachen, Ger., International DME Association; 2018.
[29] Muramatsu Y, Oguma M, Yanai T, Konno M. Numerical analysis of carbon monoxide formation in DME combustion. SAE Tech Pap 2011. doi: 10.4271/2011-32-0632.
[30] Willems W, Pannwitz M, Zubel M, Weber J. Oxygenated Fuels in Compression Ignition Engines. MTZ Worldw 2020;81:26–33. https://doi.org/10.1007/s38313-019-0183-0.
[31] Cung K, Moiz AA, Zhu X, Lee SY. Ignition and formaldehyde formation in dimethyl ether (DME) reacting spray under various EGR levels. Proc Combust Inst 2017;36:3605–12. https://doi.org/10.1016/j.proci.2016.07.054.
[32] Ying W, Genbao L, Wei Z, Longbao Z. Study on the application of DME/diesel blends in a diesel engine. Fuel Process Technol 2008;89:1272–80. https://doi.org/10.1016/j.fuproc.2008.05.023.
[33] Chapman EM, Boehman A, Wain K, Lloyd W, Perez JM, Stiver D, et al. Impact of DME-Diesel Fuel Blend Properties on Diesel Fuel Injection Systems. 2003.
[34] Luo Y, He Y, Liu C, Liao S. Combustion characteristics of biodiesel with different dimethyl ether blending strategies. Fuel 2023;332:126078. https://doi.org/10.1016/j.fuel.2022.126078.
[35] Sun C, Liu Y, Qiao X, Ju D, Han W, Fang X, et al. Experimental study of effects of exhaust gas recirculation and combustion mode on combustion, emission, and performance of DME-methanol-fueled turbocharged common-rail engine. Int J Energy Res 2022;46:2385–402. https://doi.org/10.1002/er.7315.
[36] Xiao H, Li H. Experimental and kinetic modeling study of the laminar burning velocity of NH3/DME/air premixed flames. Combust Flame 2022;245:112372. https://doi.org/10.1016/j.combustflame.2022.112372.
[37] Meng X, Zhang M, Zhao C, Tian H, Tian J, Long W, et al. Study of combustion and NO chemical reaction mechanism in ammonia blended with DME. Fuel 2022;319:123832. https://doi.org/10.1016/j.fuel.2022.123832.
[38] Peters R, Breuer JL, Decker M, Grube T, Robinius M, Samsun RC, et al. Future power train solutions for long-haul trucks. Sustain 2021;13:1–59. https://doi.org/10.3390/su13042225.
[39] Lee U, Han J, Wang M, Ward J, Hicks E, Goodwin D, et al. Well-to-Wheels Emissions of Greenhouse Gases and Air Pollutants of Dimethyl Ether from Natural Gas and Renewable Feedstocks in Comparison with Petroleum Gasoline and Diesel in the United States and Europe. SAE Int J Fuels Lubr 2016;9:546–57. https://doi.org/10.4271/2016-01-2209.
[40] Poulikidou S, Heyne S, Grahn M, Harvey S, Hansson J. A Comparative Assessment of Current and Future Fuels for the Transport Sector. Eur Biomass Conf Exhib 2018:1396–407.
[41] N/N. Proposal for Regulation of the European Parliament and of the Council on Type-Approval of Motor Vehicles and Engine of such Systems, Components and Separate Technical Units Intended for Such Vehicles, with Respect to thir Emissione and Battery Durability . vol. 2022. 2022.
[42] Salsing H, Denbratt I. Performance of a heavy duty DME diesel engine - An experimental study. SAE Tech Pap 2007;2007. https://doi.org/10.4271/2007-01-4167.
[43] Tsuchiya T, Sato Y. Development of DME engine for heavy-duty truck. SAE Tech Pap 2006. doi: 10.4271/2006-01-0052.
[44] Hara T, Shimazaki N, Yanagisawa N, Seto T, Takase S, Tokumaru T, et al. Study of DME diesel engine for Low NOx and CO2 emission and development of DME trucks for commercial use. SAE Tech Pap 2011. https://doi.org/10.4271/2011-01-1961.
[45] Fleisch T, McCarthy C, Basu A, Udovich C, Charbonneau P, Slodowske W. A New Clean Diesel Technology: Demonstration of ULEV Emissions on a Navistar Diesel Engine Fueled with Dimethyl Ether. Int. Congr. Expo., SAE International 1995. https://doi.org/10.4271/950061.
[46] Giechaskiel B, Clairotte M. Fourier transform infrared (Ftir) spectroscopy for measurements of vehicle exhaust emissions: A review. Appl Sci 2021:11. https://doi.org/10.3390/app11167416.

[47] Madia G, Koebel M, Elsener M, Wokaun A. Side reactions in the selective catalytic reduction of NOx with various NO2 fractions. Ind Eng Chem Res 2002;41:4008–15. https://doi.org/10.1021/ie020054c.
[48] Wang J, Cui H, Dong X, Zhao H, Wang Y, Chen H, et al. N2O formation in the selective catalytic reduction of NOx with NH3 on a CeMoOx catalyst. Appl Catal A Gen 2015;505:8–15. https://doi.org/10.1016/j.apcata.2015.07.030.
[49] Zhu M, Lai JK, Wachs IE. Formation of N2O greenhouse gas during SCR of NO with NH3 by supported vanadium oxide catalysts. Appl Catal B Environ 2018;224:836–40. https://doi.org/10.1016/j.apcatb.2017.11.029.
[50] Wang A, Wang Y, Walter ED, Kukkadapu RK, Guo Y, Lu G, et al. Catalytic N2O decomposition and reduction by NH3 over Fe/Beta and Fe/SSZ-13 catalysts. J Catal 2018;358:199–210. https://doi.org/10.1016/j.jcat.2017.12.011.
[51] Eck M, Lott P, Schweigert D, Börnhorst M, Deutschmann O. Spatially Resolved Measurements of HNCO Hydrolysis over SCR Catalysts. Chem-Ing-Tech 2022;94:738–46. https://doi.org/10.1002/cite.202100192.
[52] Al-Rawashdeh H, Hasan AO, Gomaa MR, Abu-jrai A, Shalby M. Determination of Carbonyls Compound, Ketones and Aldehydes Emissions from CI Diesel Engines Fueled with Pure Diesel/Diesel Methanol Blends. Energies 2022:15. https://doi.org/10.3390/en15217933.